

# Gerasimov-Drell-Hearn Sum Rule and the Discrepancy between the New CLAS and SAPHIR Data

T. Mart\*

Departemen Fisika, FMIPA, Universitas Indonesia, Depok, 16424, Indonesia

October 31, 2018

## ABSTRACT

Contribution of the  $K^+\Lambda$  channel to the Gerasimov-Drell-Hearn (GDH) sum rule has been calculated by using the models that fit the recent SAPHIR or CLAS differential cross section data. It is shown that the two data sets yield quite different contributions. Contribution of this channel to the forward spin polarizability of the proton has been also calculated. It is also shown that the inclusion of the recent CLAS  $C_x$  and  $C_z$  data in the fitting data base does not significantly change the result of the present calculation. Results of the fit, however, reveal the role of the  $S_{11}(1650)$ ,  $P_{11}(1710)$ ,  $P_{13}(1720)$ , and  $P_{13}(1900)$  resonances for the description of the  $C_x$  and  $C_z$  data. A brief discussion on the importance of these resonances is given. Measurements of the polarized total cross section  $\sigma_{TT'}$  by the CLAS, LEPS, and MAMI collaborations are expected to verify this finding.

PACS : 14.40.Aq, 13.40.Gp, 25.30.Rw

---

\*E-mail address: tmart@fisika.ui.ac.id

# 1 INTRODUCTION

The two sets of ample, good quality, experimental data of kaon photoproduction  $\gamma p \rightarrow K^+ \Lambda$  provided recently by the SAPHIR [1] and CLAS [2] collaborations lead to not only a new opportunity to study the dynamics of kaon and hyperon interactions in a great detail, but also a puzzling point: Why there exist discrepancies between the two data sets in the  $\gamma p \rightarrow K^+ \Lambda$  channel, whereas in the  $\gamma p \rightarrow K^+ \Sigma^0$  channel the extracted data from the two collaborations agree quite well? Many recent efforts have been devoted to analyze the consequence of the data discrepancies in the  $\gamma p \rightarrow K^+ \Lambda$  process (see e.g., [3, 4, 6]). It is shown by Refs. [4, 5] that the use of SAPHIR and CLAS data, individually or simultaneously, leads to quite different extracted photo-coupling parameters. Therefore, Ref. [4] concluded that current data situation does not allow for a precise determination of the resonance parameters or for the search of the “missing resonances”.

By studying the statistical properties of the two data sets Ref. [6] showed that the CLAS data are in good agreement with the LEPS data [7], whereas the SAPHIR data are coherently shifted down with respect to both CLAS and LEPS data, especially at forward kaon angles. The relative-global-scaling factor between the SAPHIR and CLAS data has been found to be 1.13.

Although results of the recent works could reveal certain consequences of using SAPHIR or CLAS data in the database, it is still difficult to determine which data set should be used to obtain a reliable phenomenological model as well as to extract the correct resonance parameters. The reason is that in all analyses the experimental data are fitted by adjusting a set of free parameters, while the precise values of these parameters are not well known. Furthermore, the extracted parameters are not unique and also sensitive to the number of resonances used in a model. Here, it is important to note that due to the high-energy threshold it is difficult to identify which resonances are dominant in this reaction.

In view of this, it is important to consider other quantities which can be predicted by the models and can be directly compared with the results from other measurements or model predictions. One of the possible quantities is the contribution of the  $\gamma p \rightarrow K^+ \Lambda$  channel to the Gerasimov-Drell-Hearn (GDH) sum rule. Previous calculations based on isobar models [8, 9, 10, 11] have estimated that kaon photoproductions on the proton contribute about  $+4 \mu\text{b}$  to the GDH integral. Actually, to arrive at a correct GDH sum rule prediction one merely needs about  $+2 \mu\text{b}$  contribution from kaon-hyperon final states (see Table I of Ref. [10]).

Recently, the CLAS collaboration released a set of experimental data on the beam-recoil polarization observables  $C_x$  and  $C_z$  [12]. These data indicate that the  $\Lambda$  polarization is predominantly in the direction of the spin of the incoming photon, independent of the c.m. energy or the kaon scattering angle. By using a circularly polarized photon beam the polarization of the recoiling hyperon is measured. The measured polarization is defined through the relation

$$R_\Lambda = \sqrt{P_\Lambda^2 + C_x^2 + C_z^2}, \quad (1)$$

where  $P_\Lambda$  is the induced (recoil) polarization of the hyperon. We note that for a circularly polarized beam this polarization is bounded to be less than or equal to one [13]. When integrated over all production angles and total c.m. energies, the CLAS data gives

$$R_\Lambda = 1.01 \pm 0.01 .$$

However, this result seems to be difficult to explain. Reference [14] tried to explain this phenomenon by means of a simple quark model. Within this approach, the real photon converts to an  $s\bar{s}$  pair as part of the interaction in the complex gluon field of the nucleon. The pair carries the polarization of the photon. The  $s$  quark of the pair merges with the  $ud$  quarks of the proton to form a  $\Lambda$ . The  $s$  quark in the  $\Lambda$  retains its full polarization after being precessed by a spin-orbit interaction, while the  $\bar{s}$  quark merges with the remnant  $u$  quark and ends up in the spinless kaon. Using this model Ref. [14] is able to qualitatively explain the phenomenon. However, as pointed out by Ref. [15], in this approach the  $s$ -channel baryon resonances cannot play an important role, since the  $s\bar{s}$  pair is created in the initial state. This is in contrary to the fact that kaon photoproduction is dominated by the resonance contributions. Moreover, the approach is unable to reproduce the qualitative features of the  $\gamma p \rightarrow K^+\Sigma^0$  process [15]. Based on these facts, it is certainly interesting to include the CLAS  $C_x$  and  $C_z$  data in the present analysis and to investigate the effects of the data inclusion.

This paper is organized as follows. In Section 2 we present the formalism of the GDH sum rule. Section 3 briefly explains the multipole model used in the data analysis. Section 4 presents the results before we include the CLAS  $C_x$  and  $C_z$  data in our analysis. The effect of the inclusion of these data will be demonstrated in Section 5. We will summarize our findings in Section 6.

## 2 THE GDH SUM RULE

The GDH sum rule [16] relates the anomalous magnetic moment of the nucleon  $\kappa_N$  to the difference of its polarized total photoabsorption cross sections. For the case of proton the sum rule reads

$$-\frac{\kappa_p^2}{4} = \frac{m_p^2}{8\pi^2\alpha} \int_{E_\gamma^{\text{thr}}}^{\infty} \frac{dE_\gamma}{E_\gamma} \left[ \sigma_{1/2}(E_\gamma) - \sigma_{3/2}(E_\gamma) \right], \quad (2)$$

where  $\sigma_{3/2}$  and  $\sigma_{1/2}$  indicate the cross sections for the possible combinations of spins of the proton (1/2) and the photon (1),  $E_\gamma^{\text{thr}}$  the photoproduction threshold lab energy,  $\alpha = e^2/4\pi = 1/137$  the fine structure constant, and  $m_p$  the proton mass.

For unpolarized photoproduction experiments the total cross section  $\sigma_T$  can be related to the spin dependent cross sections by

$$\sigma_T = \frac{1}{2} (\sigma_{3/2} + \sigma_{1/2}), \quad (3)$$

while for the photoproduction from the polarized photon beam and polarized proton target,

$$\vec{\gamma} + \vec{p} \rightarrow K^+ + \Lambda, \quad (4)$$

one can also measure

$$\sigma_{\text{TT}'} = \frac{1}{2} (\sigma_{3/2} - \sigma_{1/2}). \quad (5)$$

The latter is obviously the suitable observable for the sum rule. However, since there has been no available measurement of the reaction given in Eq. (4) yet, Eq. (5) should be estimated from a reliable model which fits all available unpolarized experimental data.

For the sake of comparison, we follow the notation of Ref. [10] and define the GDH integral

$$I_{\text{GDH}} \equiv \int_{E_\gamma^{\text{thr}}}^{\infty} \frac{dE_\gamma}{E_\gamma} \left[ \sigma_{1/2}(E_\gamma) - \sigma_{3/2}(E_\gamma) \right]. \quad (6)$$

With this definition, the GDH sum rule for the proton yields

$$I_{\text{GDH}} = -\frac{2\pi^2\alpha\kappa^2}{m_p^2} = -204.5 \mu\text{b}. \quad (7)$$

The first estimate based on the then existing data led to  $I_{\text{GDH}} = -261 \mu\text{b}$  [17]. The latest result calculated from a combination of pion photoproduction and photon absorption processes yields a value of  $-211 \pm 15 \mu\text{b}$  [18], thus, although it slightly overestimates the sum rule, it is still consistent within the present error bar. However, one can also calculate the  $I_{\text{GDH}}$  by summing up all possible photoproduction processes. This was done in Ref. [10], and it is found that in order to arrive at a consistent result, an estimate of  $+4 \mu\text{b}$  contribution should come from kaon photoproduction processes on the proton. By using KAON-MAID it can be shown that a slightly smaller value of  $1.25 + 1.38 + 0.30 = 2.93 \mu\text{b}$  can be expected from these associated strangeness processes, where the three separate contributions refer to the  $K^+\Lambda$ ,  $K^+\Sigma^0$ , and  $K^0\Sigma^+$  channels [11]. The small contribution from the  $K^0\Sigma^+$  channel can be understood from the fact that the cross section of this channel is substantially smaller than those of the  $K^+\Lambda$  and  $K^+\Sigma^0$  channels (see, e.g., Ref. [19]). The latest measurement of the  $K^0\Sigma^+$  channel [20] shows that the corresponding cross section is even smaller than that reported in Ref. [19]. This indicates that the contribution of the kaon-hyperon final states to the GDH sum rule for the case of the proton probably comes only from the  $K^+\Lambda$  and  $K^+\Sigma^0$  channels.

With the knowledge of  $\sigma_{\text{T}T'}$  we can also calculate the corresponding contribution to the forward spin polarizability of the proton,

$$\gamma_0 = \frac{1}{4\pi^2} \int_{E_\gamma^{\text{thr}}}^{\infty} \frac{dE_\gamma}{E_\gamma^3} \left[ \sigma_{1/2}(E_\gamma) - \sigma_{3/2}(E_\gamma) \right]. \quad (8)$$

The precise value of this observable is currently less known, since there is no sign that calculations from Chiral Perturbation Theory (ChPT) would converge in this case. For instance, the isobar model of Ref. [10] predicts  $\gamma_0 = -0.65$  (in  $10^{-4} \text{fm}^4$ ), whereas the analysis from ChPT to order  $\mathcal{O}(p^3)$  obtains a value of 4.6 [21] and an extension to  $\mathcal{O}(p^4)$  yields  $-3.9$  [22]. The latest value obtained from photoabsorption experiment [18] is  $-0.94 \times 10^{-4} \text{fm}^4$ . In spite of this enormous uncertainty it is important to note that Ref. [10] estimates a small contribution from the  $n\pi + \eta$  channels, i.e.  $-0.01 \times 10^{-4} \text{fm}^4$ , in spite of the fact that the  $n\pi$  channel could have total a cross section up to five orders of magnitude larger than that of kaon channels.

### 3 THE MULTIPOLE MODEL

One of the most recent models of the  $K^+\Lambda$  photoproduction which fits all recent-experimental data, in a wide range of kinematics, from threshold up to  $E_\gamma \approx 3 \text{ GeV}$  is the recent multipole

model given in Ref. [4]. The model consists of the background terms which are constructed from a series of tree-level Feynman diagrams and the resonance terms which are assumed to have the Breit-Wigner form. To account for hadronic structures of interacting baryons and mesons the appropriate hadronic form factors are included in hadronic vertices in a gauge-invariant fashion. Details of the ingredient of the model can be found in Ref. [4]. A number of free parameters in the background and resonance terms are adjusted by fitting the calculated observables to experimental data. Due to the problem of the data discrepancies, two models have been proposed in Ref. [4]. The first model fits the combination of the SAPHIR and LEPS data (hereafter referred to as Fit 1a) and the second one fits the combination of the CLAS and LEPS data (hereafter referred to as Fit 2a). Before the inclusion of the CLAS beam-recoil polarization data  $C_x$  and  $C_z$ , in total, 834 data points were fitted in the first case and 1694 data points were fitted in the second case. To further analyze the physical consequence of the data discrepancy, we have refitted this multipole model solely to the SAPHIR data (750 data points) or CLAS data (1377 data points). The results are referred to as Fit 1 (fits to the SAPHIR data) and Fit 2 (fits to the CLAS data). The CLAS beam-recoil polarization data  $C_x$  and  $C_z$  consists of 320 data points. The results after the inclusion of these data will be presented in Section 5.

## 4 CONTRIBUTION TO THE GDH SUM RULE

Figure 1 displays the comparison between the predicted total cross sections  $\sigma_T$  and experimental data in the upper panel. Predictions for the  $\sigma_{TT'}$  total cross section are given in the lower panel of the same figure. For the sake of completeness, we also present the prediction of KAON-MAID (indicated by Maid in the figure).

Since the number of experimental data used in the new fits (Fit 1 and Fit 2) is smaller, it is understandable that the agreement between experimental data and model predictions is better in this case. The predictions for the  $\sigma_{TT'}$  show, however, quite different behaviors for different models. The differences between Fit 1 and Fit 1a (as well as between Fit 2 and Fit 2a) originate from the differences in the fitted (resonance) parameters, thus, reflecting the differences in the resonance roles in explaining the process. Nevertheless, the gross behaviors of Fit 1 and Fit 1a are almost the same. The same feature is also displayed by Fit 2 and Fit 2a. The main difference is, whereas Fit 1 and Fit 1a do not cross the zero axis, Fit 2 and Fit 2a change their signs at  $E_\gamma \approx 1.2$  GeV. Based on this result we can then expect smaller  $I_{GDH}$  values in the case of Fit 2 and Fit 2a (the case of using CLAS data).

The negative and small values of  $\gamma_0$  predicted by Fit 2 and Fit 2a, respectively, are also expected, since the integrands of Eqs. (6) and (8) are similar up to the power in the denominator.

The numerical results of the  $I_{GDH}$  shown in Table 1 prove our expectations. To help to understand these numerical values we present the evolutions of the integrands of Eqs. (6) and (8) in Fig. 2. The predicted  $I_{GDH}$  of Fit 1 and Fit 1a are much closer to the MAID prediction than those of Fit 2 and Fit 2a, indicating the consistency of the new SAPHIR data [1] to the old ones [23]. The origin of the negative values obtained from Fit 2 and Fit 2a is obvious from the evolution of both integrands shown by the dotted and dashed curves in the upper panel of Fig. 2.

It comes as no surprise that the predicted values of  $\gamma_0$  are quite small compared to the

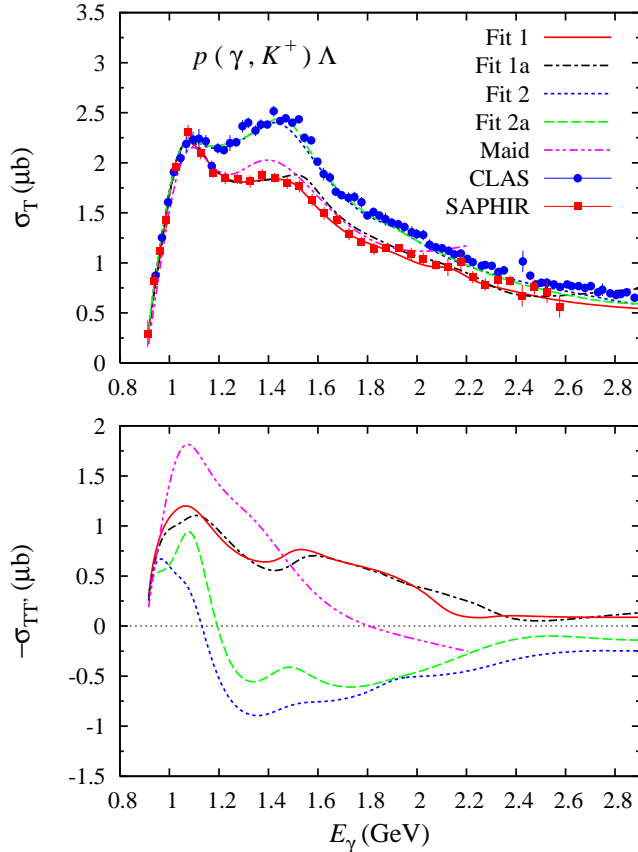


FIGURE 1: (Color online) Total cross sections  $\sigma_T$  (upper panel) and  $-\sigma_{TT'}$  (lower panel) for the  $\gamma p \rightarrow K^+\Lambda$  channel plotted as a function of the photon laboratory energy  $E_\gamma$ . Fit 1a and Fit 2a show the result of a multipole analysis of Ref. [4] that fits SAPHIR and CLAS data, respectively. Fit 1 and Fit 2 demonstrate the result of the same multipole analysis, but refitted solely to the SAPHIR and CLAS data, respectively. The prediction of the KAON-MAID model is indicated in both panels by Maid. Solid squares and solid circles display experimental data from the SAPHIR [1] and the CLAS [2] collaborations, respectively. Note that all data shown in this figure were not used in the fits.

presently known value, i.e.,  $-0.94 \times 10^{-4} \text{ fm}^4$  [18]. However, it is interesting to compare the contribution from the  $n\pi + \eta$  channels, i.e.  $-1 \times 10^{-6} \text{ fm}^4$ , to those predicted by both Fit 1 and Fit 1a (as well as MAID), i.e.  $\gamma_0 \approx +1 \times 10^{-7} \text{ fm}^4$ . The absolute value of the latter is one order of magnitude smaller than the former, although the total cross section  $\sigma_T$  of the latter could be five orders of magnitude smaller than the former. This result recommends a further analysis of the contribution from the  $n\pi + \eta$  channels to the  $\gamma_0$ .

The different behaviors shown by Fit 2 and Fit 2a can be traced back to the role of the background and resonance terms in these models. It is shown in Ref. [4] that, in contrast to the model that fits the SAPHIR data, model that fits the CLAS data (in this case Fit 2a) yields an unrealistically large background contribution. To overcome this, the resonance contributions

TABLE 1: Contributions of the  $\gamma p \rightarrow K^+\Lambda$  channel to the GDH sum rule for the proton in  $\mu\text{b}$  and to the forward spin polarizability  $\gamma_0$  in  $10^{-7} \text{ fm}^4$ . Note that the numerical values of the  $I_{\text{GDH}}$  refer to  $\int_{E_\gamma^{\text{thr}}}^\infty dE_\gamma (\sigma_{1/2} - \sigma_{3/2})/E_\gamma$  in Eq. (6). For comparison, the GDH sum rule yields the value of  $-204.5 \mu\text{b}$ , while Ref. [10] estimates a value of  $+4 \mu\text{b}$  for all kaon photoproduction channels on the proton. On the other hand, Ref. [10] obtains a value of  $-0.65 \times 10^{-4} \text{ fm}^4$  for the contribution from single pion photoproduction below 1.6 GeV to the  $\gamma_0$ . The number of fitted data  $N$  and the corresponding  $\chi^2$  per degrees of freedom are also given.

Observable	MAID	Fit 1	Fit 1a	Fit 2	Fit 2a
$I_{\text{GDH}} (\mu\text{b})$	1.247	1.309	1.274	-0.845	-0.333
$\gamma_0 (10^{-7} \text{ fm}^4)$	0.939	0.807	0.753	-0.208	0.060
$N$	319	720	834	1377	1694
$\chi^2/N_{\text{dof}}$	3.36	0.78	1.02	0.84	0.98

should produce a kind of destructive interference with the background terms. Another problem with the Fit 2a model is shown in Ref. [24]. In spite of the fact that Fit 2a was fitted to the CLAS photoproduction data, it fails to reproduce the CLAS electroproduction data [25]. Surprisingly, this is in contrast to the Fit 1a model, which is fitted to the SAPHIR photoproduction data.

## 5 INCLUSION OF THE $C_x$ AND $C_z$ DATA

Traditionally, the beam-recoil polarization observables are calculated in the system where the  $z'$  is defined by the direction of the outgoing kaon [26]. The observables are therefore called by  $C_{x'}$  and  $C_{z'}$ . The CLAS collaboration measured these observables, however, in the system where the  $z$  axis of the reaction plane is along the direction of the photon beam [12]. Therefore, in our calculation we should consider  $C_x$  and  $C_z$  which can be obtained from the standard rotation matrix,

$$C_x = C_{x'} \cos \theta + C_{z'} \sin \theta , \quad (9)$$

$$C_z = -C_{x'} \sin \theta + C_{z'} \cos \theta , \quad (10)$$

where  $\theta$  is the kaon scattering angle. For the definition of  $C_{x'}$  and  $C_{z'}$  we follow Refs. [12, 15].

After including the CLAS  $C_x$  and  $C_z$  data in the fitting database we refit the Fit 1, Fit 1a, Fit 2, and Fit 2a models and denote the refitted models by Fit 1x, Fit 1ax, Fit 2x, and Fit 2ax. As shown in Figs. 3–6 the agreement between the calculated and the experimental data of  $C_x$  and  $C_z$  can be satisfactorily achieved. We also find that in order to fit these data we do not need a weighting factor as in Ref. [15]. This is clearly demonstrated by the agreement of the calculated and experimental data of  $C_x$  and  $C_z$  as well as the  $\chi^2/N_{\text{dof}}$  listed in Table 2, where in all cases the latter increases only slightly. At higher  $W$  all models start to vary, because experimental data at this kinematics have large error bars. The disagreement of KAON-MAID with the recent CLAS  $C_x$  and  $C_z$  data is expected, since this model has very few nucleon resonances and was fitted to a small number of experimental data

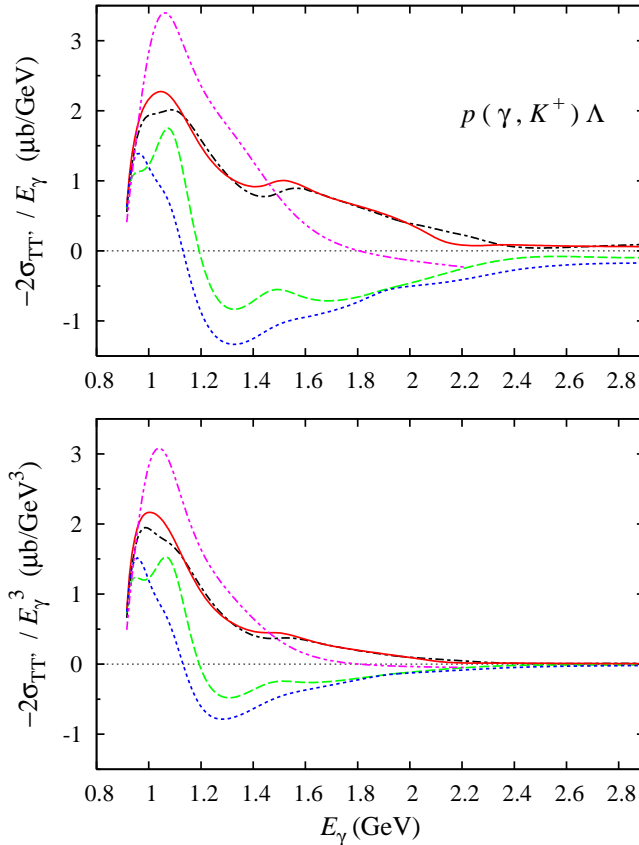


FIGURE 2: (Color online) The integrands of Eq. (6) (upper panel) and Eq. (8) (lower panel) for all five models given in Table 1 as a function of the photon laboratory energy  $E_\gamma$ . Notation for the curves is as in Fig. 1.

The total cross sections  $\sigma_T$  and  $\sigma_{TT'}$  of the refitted models display an interesting result. As shown in Fig. 7, the inclusion of the  $C_x$  and  $C_z$  data emphasizes our previous finding; the models which fitted the CLAS differential cross section data predicts a (more) negative contribution to the GDH sum rule. The numerical results given in Table 2 show this explicitly. Given that there is no discrepancy between the SAPHIR and CLAS  $K^+\Sigma^0$  data, so that the previous result of the  $K^+\Sigma^0$  channel is still valid, and the contribution of the  $K^0\Sigma^+$  channel can be neglected, we can conclude that models which fit the CLAS differential cross section data (Fit 2x and Fit 2ax) tend to eliminate the contribution of kaon-hyperon final states to the GDH sum rule.

It is also important to briefly discuss the differences between the predicted  $\sigma_{TT'}$  before and after the inclusion of the  $C_x$  and  $C_z$  data (shown in the lower panels of Figs. 1 and 7). After the inclusion of the beam-recoil data the total cross sections  $\sigma_{TT'}$  show less structures. Presumably, the CLAS  $C_x$  and  $C_z$  data select certain resonances as the important ones. To investigate this, in Fig. 8 we plot contributions of the background terms and several important resonances to the



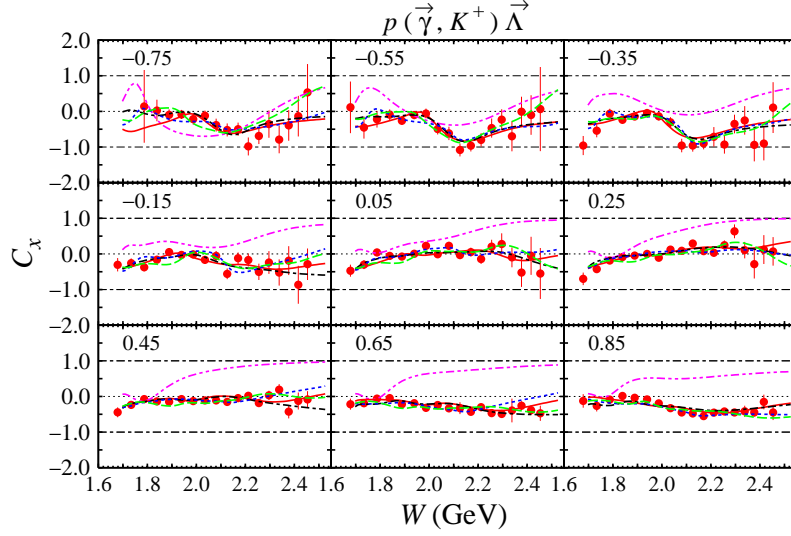


FIGURE 3: (Color online) The beam-recoil observable  $C_x$  for the reaction  $\bar{\gamma}p \rightarrow K^+\bar{\Lambda}$  plotted as a function of the total c.m. energy  $W$ . Experimental data are taken from Ref. [12]. The corresponding value of  $\cos\theta$  is shown in each panel. Notation of the curves is as in Fig. 1.

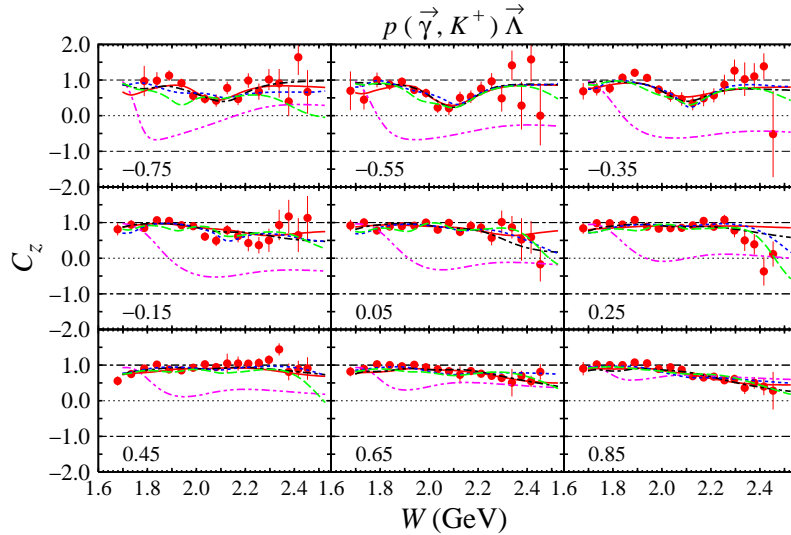


FIGURE 4: (Color online) As in Fig. 3, but for the observable  $C_z$ .

total cross section  $\sigma_{\text{TOT}}$  before and after the inclusion of the beam-recoil observables. Although the phenomenon is observed in all four fits, we only compare Fit 1a and Fit 1ax because the effect of the  $C_x$  and  $C_z$  inclusion is more dramatic in this case.

By comparing the upper and lower panels of Fig. 8 we can conclude that the inclusion of

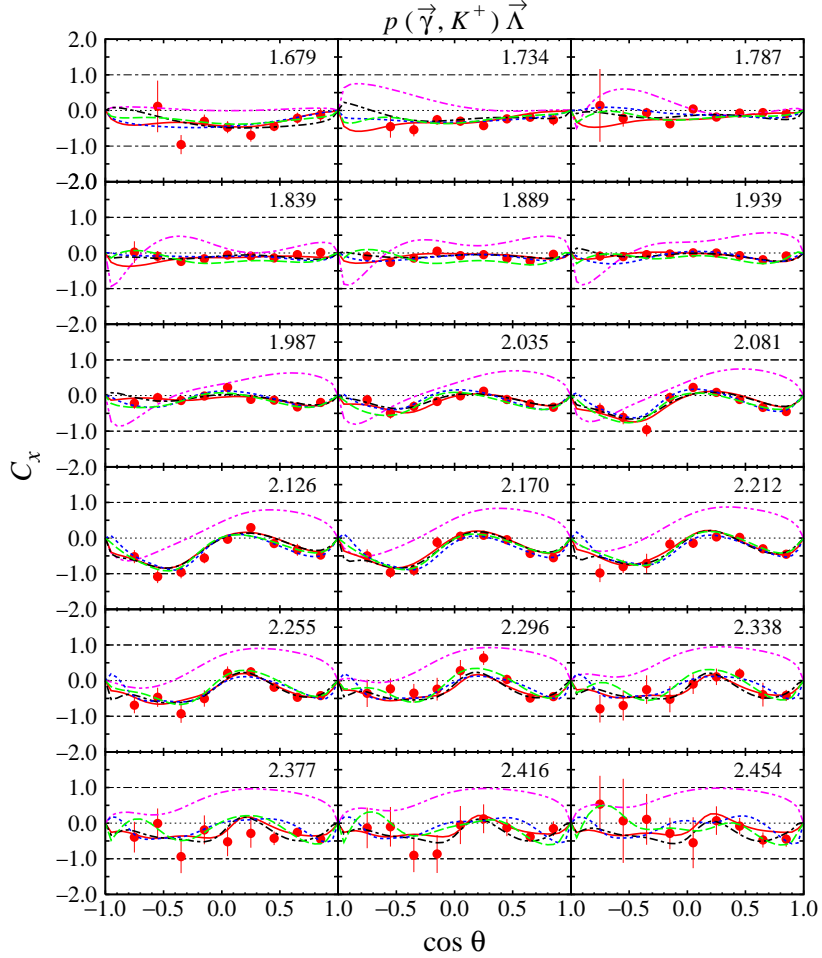


FIGURE 5: (Color online) The beam-recoil observable  $C_x$  plotted as a function of the kaon scattering angle. Notations of the curves and experimental data are as in Fig. 3. Shown in each panel is the total c.m. energy  $W$  in GeV.

the  $C_x$  and  $C_z$  data does not influence the background sector of the model. In the resonance sector, this inclusion emphasizes the roles of the  $S_{11}(1650)$ ,  $P_{11}(1710)$ ,  $P_{13}(1720)$ , and  $P_{13}(1900)$  resonances. The result of the present work, therefore, corroborates the finding of the authors of Ref. [15] about the evidence of the  $P_{13}(1900)$  resonance, who also used the CLAS  $C_x$  and  $C_z$  data in their analysis. We note that this analysis has been further reexamined in a great detail in Ref. [27], where it is shown that the  $P_{13}(1900)$  resonance is essential to achieve a good quality of the fit, especially for the  $C_x$  and  $C_z$  data. It is also important to note that Ref. [4] has pointed out that this resonance is important if the CLAS differential cross section data were used. With the same quantum states, another important resonance is the  $P_{13}(1720)$ . Reference [27] also found that this resonance belongs to the four strongest contributors to the  $\gamma p \rightarrow K^+ \Lambda$  reaction. The importance of the  $S_{11}(1650)$  in the photoproduction of  $K^+ \Lambda$  is quite clear because the

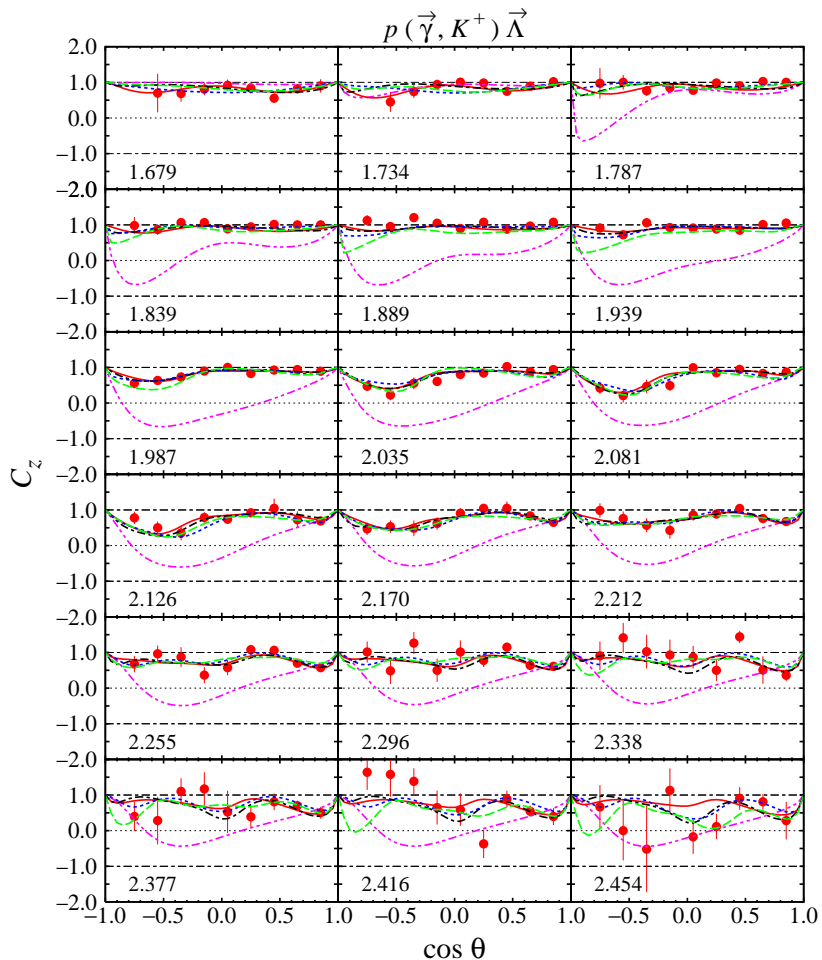


FIGURE 6: (Color online) As in Fig. 5, but for the observable  $C_z$ .

$s$ -wave contribution dominates the threshold of this process [23]. This has been also discussed in the previous works [1, 4, 15].

Apparently, the only different result obtained here is the importance of the  $P_{11}(1710)$  state. Most recent studies [3, 4, 15, 28] found that this resonance has a negligible effect on the  $\gamma p \rightarrow K^+\Lambda$  reaction, in spite of the fact that this resonance has long been used in the isobar models of kaon photoproduction [29]. Although its contribution could be smaller than those of the  $S_{11}(1650)$ ,  $P_{13}(1720)$ , and  $P_{13}(1900)$  resonances, Fig. 8 recommends that a further detailed study of the  $C_x$  and  $C_z$  data is urgently required to shed more light on the role of the  $P_{11}(1710)$  state.

Finally, we should mention that due to the nature of the prediction here, experimental measurement of the  $\sigma_{TT'}$  is urgently required to verify the current findings. Since the SAPHIR detector has been dismantled, measurements of the  $\sigma_{TT'}$  by the CLAS, LEPS, and MAMI collaborations seem to be the only choice.

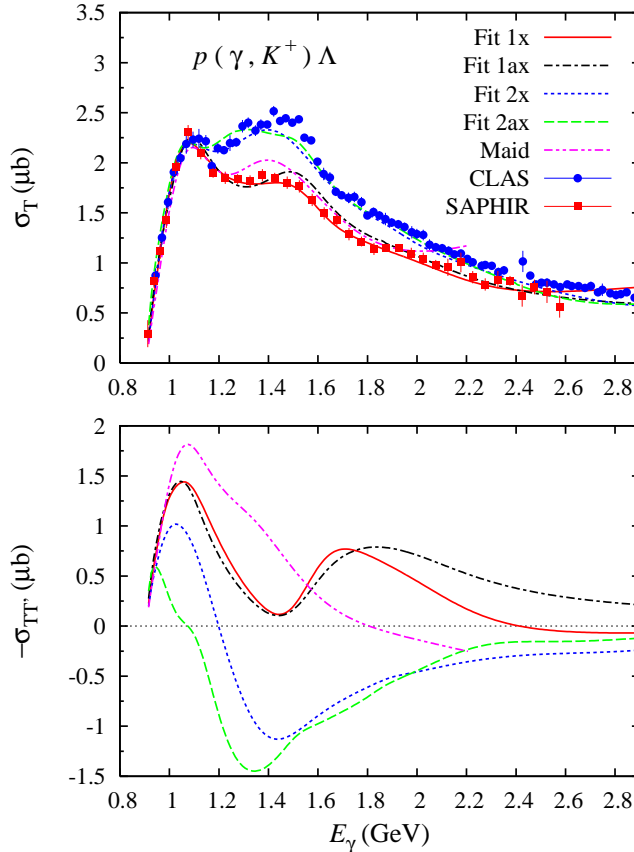


FIGURE 7: (Color online) As in Fig. 1, but all curves (except those of Kaon-Maid) are obtained from the same models which have been refitted after the inclusion of the beam-recoil polarization data  $C_x$  and  $C_z$  in the fitting database.

## 6 CONCLUSION

In conclusion, we have calculated the contribution of the kaon photoproduction  $\gamma p \rightarrow K^+ \Lambda$  channel to the GDH sum rule by means of multipole models which fit the new SAPHIR or CLAS data. Our findings indicate that the SAPHIR and CLAS data yield very different contributions to the GDH sum rule. Contribution of this channel to the forward spin polarizability of the proton recommends a further analysis of the contribution from the  $n\pi + \eta$  channels. The inclusion of the recent CLAS  $C_x$  and  $C_z$  data does not dramatically change this conclusion. The result of the fits that include these data supports the previous finding that the  $S_{11}(1650)$ ,  $P_{13}(1720)$ , and  $P_{13}(1900)$  resonances are essential for the  $K^+ \Lambda$  photoproduction. Future measurements of the  $\sigma_{TT'}$  by the CLAS, LEPS, and MAMI collaborations, are expected to confirm this conclusion.

The author acknowledges the support from the University of Indonesia.

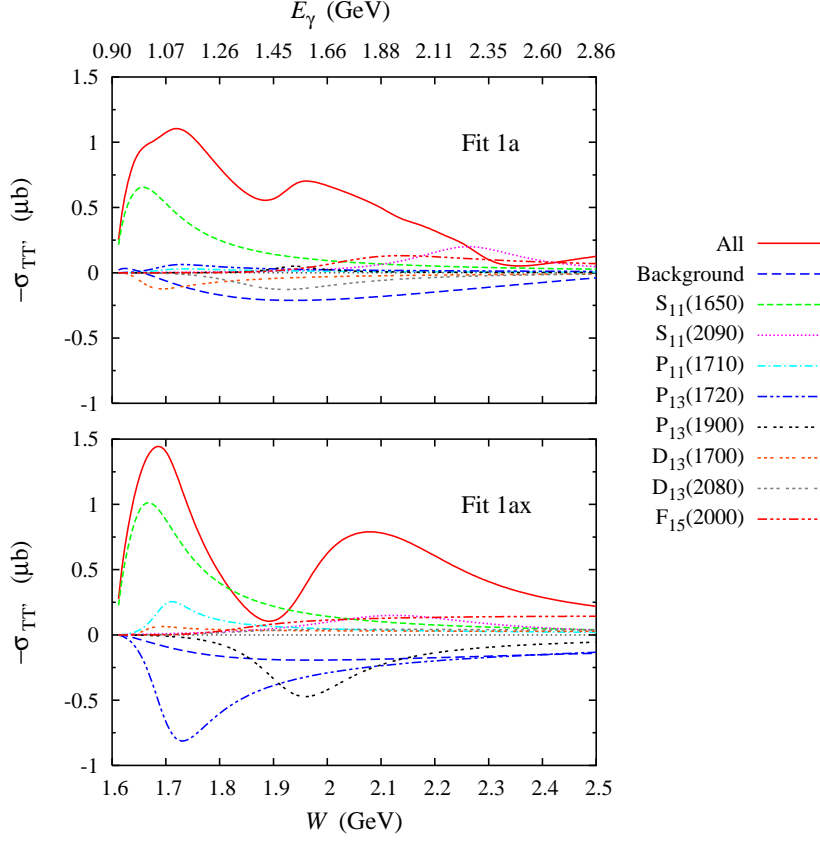


FIGURE 8: (Color online) Contribution of the background terms and several important resonances to the total cross section  $\sigma_{\text{TT}'}$  before (Fit 1a) and after (Fit 1ax) the inclusion of the beam-recoil polarization observables  $C_x$  and  $C_z$ . The total cross sections  $\sigma_{\text{TT}'}$  obtained by including all terms are indicated by the solid lines. Note that contributions from other resonances are small and, therefore, are not shown in this figure for the sake of clarity.

## REFERENCES

- [1] K. H. Glander *et al.*, *Eur. Phys. J. A* **19**, 251 (2004).
- [2] R. Bradford *et al.*, *Phys. Rev. C* **73**, 035202 (2006).
- [3] B. Julia-Diaz, B. Saghai, T. S. Lee and F. Tabakin, *Phys. Rev. C* **73**, 055204 (2006).
- [4] T. Mart and A. Sulaksono, *Phys. Rev. C* **74**, 055203 (2006).
- [5] A. V. Sarantsev, V. A. Nikonov, A. V. Anisovich, E. Klempt and U. Thoma, *Eur. Phys. J. A* **25**, 441 (2005).
- [6] P. Bydzovsky and T. Mart, *Phys. Rev. C* **76**, 065202 (2007).

TABLE 2: As in Table 1, but obtained after the inclusion of the  $C_x$  and  $C_z$  data. Note that the result of KAON-MAID has been excluded from this Table.

Observable	Fit 1x	Fit 1ax	Fit 2x	Fit 2ax
$I_{\text{GDH}} (\mu\text{b})$	1.140	1.380	-0.642	-1.181
$\gamma_0 (10^{-7} \text{ fm}^4)$	0.752	0.785	-0.033	-0.466
$N$	1040	1154	1697	2014
$\chi^2/N_{\text{dof}}$	0.93	1.13	0.91	1.28

- [7] M. Sumihama *et al.*, Phys. Rev. C **73**, 035214 (2006).
- [8] H.-W. Hammer, D. Drechsel, and T. Mart, nucl-th/9701008, 1997
- [9] S. Sumowidagdo and T. Mart, Phys. Rev. C **60**, 028201 (1999).
- [10] D. Drechsel, S. S. Kamalov, and L. Tiator, Phys. Rev. D **63**, 114010 (2001). For a previous result see D. Drechsel, S. S. Kamalov, G. Krein, and L. Tiator, Phys. Rev. D **59**, 094021 (1999).
- [11] T. Mart, Int. J. Mod. Phys. A **23**, 599 (2008).
- [12] R. Bradford *et al.*, Phys. Rev. C **75**, 035205 (2007).
- [13] X. Artru, J. M. Richard and J. Soffer, Phys. Rev. C **75**, 024002 (2007).
- [14] R. Schumacher, “Polarization of hyperons in elementary photoproduction,” arXiv:nucl-ex/0611035.
- [15] A. V. Anisovich, V. Kleber, E. Klempt, V. A. Nikonov, A. V. Sarantsev and U. Thoma, Eur. Phys. J. A **34**, 243 (2007).
- [16] S.B. Gerasimov, Sov. J. Nucl. Phys. **2**, 430 (1966); S.D. Drell and A.C. Hearn, Phys. Rev. Lett. **16**, 908 (1966).
- [17] I. Karliner, Phys. Rev. D **7**, 2717 (1973).
- [18] D. Drechsel and T. Walcher, arXiv:0711.3396 [hep-ph].
- [19] R. Lawall *et al.*, Eur. Phys. J. A **24**, 275 (2005).
- [20] R. Castelijns *et al.*, “Nucleon resonance decay by the  $K^0\Sigma^+$  channel,” arXiv:nucl-ex/0702033.
- [21] V. Bernard, N. Kaiser, and U.-G. Meißner, Int. J. Mod. Phys. E **4**, 193 (1995).
- [22] X. Ji, C.-W. Kao, and J. Osborne, Phys. Lett. B **472**, 1 (2000); K. B. V. Kumar, J. A. McGovern, and M. Birse, hep-ph/9909442 (1999).

- [23] M. Q. Tran *et al.*, Phys. Lett. B **445**, 20 (1998).
- [24] T. Mart and A. Sulaksono, in *Proceedings of the IX International Conference on Hypernuclear and Strange Particle Physics HYP2006, Mainz, 2006*, edited by J. Pochodzalla and Th. Walcher (Springer-Verlag, Italy, 2007) p. 345; arXiv:nucl-th/0701007.
- [25] P. Ambrozewicz *et al.*, Phys. Rev. C **75**, 045203 (2007).
- [26] G. Knöchlein, D. Drechsel, and L. Tiator, Z. Phys. A 352 (1995) 327.
- [27] V. A. Nikonov, A. V. Anisovich, E. Klempt, A. V. Sarantsev and U. Thoma, “Further evidence for  $N(1900) P_{13}$  from photoproduction of hyperons,” arXiv:0707.3600 [hep-ph].
- [28] R. A. Arndt, Y. I. Azimov, M. V. Polyakov, I. I. Strakovsky and R. L. Workman, Phys. Rev. C **69**, 035208 (2004).
- [29] R. A. Adelseck, C. Bennhold and L. E. Wright, Phys. Rev. C **32**, 1681 (1985); R. A. Adelseck and B. Saghai, Phys. Rev. C **42**, 108 (1990); R. A. Williams, C. R. Ji and S. R. Cotanch, Phys. Rev. C **43**, 452 (1991); T. Mart and C. Bennhold, Phys. Rev. C **61**, 012201 (2000); T. Mart, Phys. Rev. C **62**, 038201 (2000); T. Mart, C. Bennhold and C. E. Hyde-Wright, Phys. Rev. C **51**, 1074 (1995).